Optimal Planning of Battery Energy Storage Systems for Mitigating Voltage Fluctuations in Active Distribution Networks

Khawaja Khalid Mehmood, Saad Ullah Khan, Zunaib Maqsood Haider, Soon-Jeong Lee, Muhammad Kashif Rafique, and Chul-Hwan Kim

***Abstract*— Variations in solar irradiance and wind speed cause fluctuations in voltage of distribution networks. Battery energy storage systems (BESSs) are usually installed in the distribution networks to mitigate the effects of these voltage fluctuations. The lifespan of a BESS-battery is affected by various factors such as the operating temperature, the level of depth of discharge and the magnitude of charging and discharging currents. In this paper, a new methodology is proposed in which the factors affecting the lifespan of the battery are modelled to find the optimal location and size of BESSs. The problem is formulated as a multi-objective optimization problem. The first objective function represents total energy losses of a distribution network, whereas the second objective function contains total investment cost associated with the installation of a BESS. Moreover, voltage regulation is carried out with the BESS. An IEEE 906 bus test feeder is used for the simulations, and both wind and solar power distributed generators are installed in the test system. The results show improvement in the voltage profile, reduction in the losses and minimized cost of installation.**

***Keywords*: Battery energy storage systems, PV panels, voltage regulation, wind power DGs.**

I. Introduction

THE integration of distributed generators (DGs) with distribution networks has increased due to the benefits associated with them. Some benefits of DGs are reduction in losses and reduction in the environmental pollution. Outputs of a few DGs such as PV panels and the wind power plants are not constant, and the variations in the wind speed and solar irradiance cause fluctuations in the voltage and frequency of the system. To mitigate the effects of these fluctuations, normally, battery energy storage systems (BESSs) are installed with them [1–3]. BESSs support the distribution networks by charging their batteries when the excessive power is available, and when the output of a DG reduces, they discharge their batteries to support the grid voltage.

This research was supported by the National Research Foundation of Korea (NRF) grant funded by the Korea government (MSIP) (No.2015R1A2A1A10052459).

K. K. Mehmood, S. U. Khan, Z. M. Haider, M. K. Rafique and C.H. Kim are with the College of Information and Communication Engineering, Sungkyunkwan University, Suwon, 440-746, South Korea. (e-mail: khalidmzd@skku.edu, saadkhan@skku.eduu, zmhaider@skku.edu, kashif@skku.edu, chkim@skku.edu).

S. J. Lee is with Economy and Management Research Institute, Korea Electric Power Corporation, Naju, Republic of Korea. (e-mail: soonjeong.lee@kepco.co.kr).

Paper submitted to the International Conference on Power Systems Transients (IPST2017) in Seoul, Republic of Korea June 26-29, 2017

The decision of selecting the size and the location of installation of a BESS is not a straightforward process as the sizes of power systems are enormous. Moreover, the lifespan of a BESS battery is affected by many factors such as the operating temperature, the magnitude of the current supplied/drawn from/to the battery and the level of depth of discharge (DOD) to which the battery is being discharged. If these factors are not considered during the sizing of the battery, they can result in high annual cost of battery replacements.

In [4], the size and location of a BESS-installation have been found. Considering the maximization of benefits for the DG owner and the utility, the accommodation of spill wind results in the reduction of annual electricity cost. In [5], a matrix real coded genetic algorithm was used to find the optimal location of a BESS-installation. The objective in this study was to minimize the cost of installation and operation of a power system. In order to maximize the utilization of wind power DGs and reduce the cost of investment, Monte Carlo simulations based method was used in [6]. In [7], a point estimate method was employed for a probability based power flow, and the optimal sizing and allocation of a BESS were made with hybrid optimization algorithm, which consisted of Tabu search and Particle swarm optimization. A Grey Wolf algorithm was used to minimize the cost of operation of a microgrid in order to find the size of a BESS in [8]. In [9] and [10], the optimal planning of BESSs was carried out considering the time-of-use prices-based schemes. In above studies, the investigators have mostly minimized the cost of operation or cost of investment to calculate the size and location of installation of a BESS. However, the factors that affect the lifespan of a BESS battery were not modelled. As mentioned earlier, the omission of the effects of these factors can cause high battery replacement costs.

In this paper, we propose a new methodology to find the size and location of a BESS placement for voltage regulation of a distribution network. The factors that shorten the lifespan of a BESS-battery are modelled and considered. The problem is formulated as a multi-objective optimization problem; the first objective function represents the power losses of the system, whereas the second objective function represents the total cost of installations associated with the BESSs. The main objective of our scheme is to achieve the regulated voltage for the distribution network. For this purpose, we also integrate a voltage regulation algorithm with the optimization algorithm.

The paper is organized as follows: Section-II presents the modelling of a BESS. In Section-III, problem formulation for the optimization algorithm is presented. Section-IV describes the test cases, and Section-V presents the results and discussion. Finally, a conclusion is given in section-VI.

II. BESS and Factors affecting its lifespan

Fluctuations in wind speed and solar irradiance generate fluctuations at the output of PV panels and wind DGs. These fluctuations directly affect the voltage and frequency of the power system, thereby degrading the power quality of the system. BESSs have proven effectiveness in reducing the effects of these variations.

A BESS consists of a battery and power conditioning systems such as inverters, filters etc. for interfacing with power systems. The battery plays an important role as it stores and releases the electrical energy as and when required. The lifespan of a BESS-battery is affected by many factors. Some of the factors are shown in Fig.1. In this study, we consider three of them namely, temperature, DOD level and magnitude of charging and discharging currents.

In the subsequent subsections, we present the models used in this study to capture the effects of these factors.

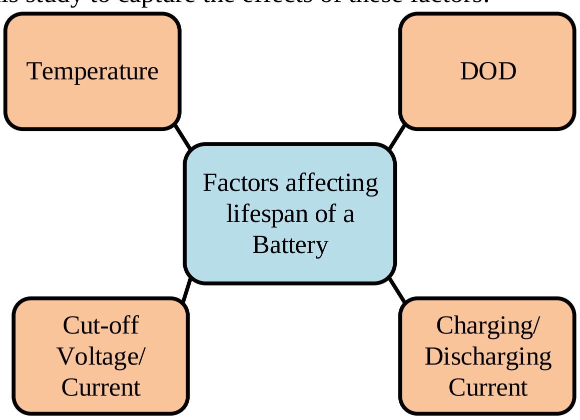

Fig. 1. Factors that affect the lifespan of a BESS-battery.

A. Temperature

The operation of a battery at both high and low temperatures affects its performance. At high temperatures, the chemical reaction inside the battery speeds up that degrades the electrodes of the battery, whereas at low temperatures, the material inside the battery is not fully activated which causes increase in the resistance that eventually reduces the lifespan of a battery. Due to the phenomenon called *capacity fading*, the total lifespan of a battery is reduced after the operation of battery at a particular temperature. Usually, capacity fade occurrence varies across the types of batteries [11].

In electric vehicles, the thermal management of a battery is a difficult task as the vehicle is moving during its operation. Installation of cooling systems requires careful thinking as the increase in the weight of the vehicle may reduce the driving range of the vehicle. However, in the case of a BESS, thermal management can easily be performed as the BESSs are stationary devices, and the installation of cooling systems can maintain a fixed operating temperature of the battery.

With the value of percentage capacity fade known, the new capacity of a battery of a particular type can be known from (1). In addition, the cost of a thermal management unit is included in the total cost of the BESS.

$$Q_{NT} = (1-\Psi_T)\times Q_r \Big|_{T=T_{op}} \tag{1}$$

where 'Q_{NT}', 'Ψ_T', 'Q_r' and 'T_{op}' are the new rated capacity of a battery after temperature fading effect, capacity fade effect of temperature, rated capacity of the battery and operating temperature, respectively. 'Q_{NT}' and 'Q_r' are measured in kWh, whereas 'Ψ_T' is in the percentage.

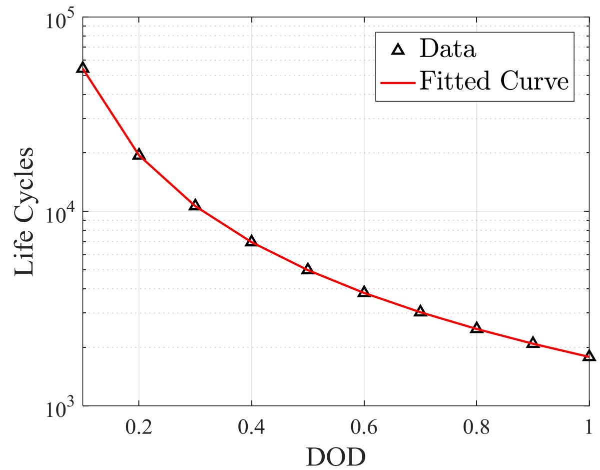

Fig. 2. Variation of life cycles with DOD

B. DOD

The lifespan of a BESS-battery is also affected by the level of DOD to which the batteries are discharged during their operations. Different studies have shown that discharging the batteries to the higher DOD level can reduce their lifespan quickly, and the lifespan can be enhanced if the batteries are discharged to a partial DOD level [12]. Fig. 2 shows the dependency of lifecycles on the DOD level for a lithium ion battery. It can be seen that as the DOD level increases, the total number of lifecycles are reduced. The fitted-curve for the data points presented in Fig. 2 can be found by using power law fitting. The parameters and equation found are given in (2). The number of lifecycles at any DOD level can be found using (2) for Li-ion batteries.

$$B_{LC} = 1783.8\times(DOD)^{-1.4832} \tag{2}$$

Where 'B_{LC}' and 'DOD' are the battery lifecycles and depth of discharge, respectively. 'DOD' is measured in percentage. For the estimation of the DOD level during the operation of the battery, we embody coulomb counting method given in (3) and (4) with the optimization algorithm [13]. The simplicity of this method reduces the execution time of the algorithm.

$$DOD(t) = DOD_{(t)} + \Delta DOD_{(t-1)} \tag{3}$$

$$\Delta DOD_{(t)}^{(b)} = \left(\frac{\int_{t_1}^{t_1+\tau} I_{Batt}^{(b)}\,dt}{Q_r^{(b)}}\right)\times 100 \tag{4}$$

Where 'I_{Batt}' is the current supplied by the battery and measured in amperes.

C. Charging and discharging current

The third factor assumed and modelled in this study is the magnitudes of charging and discharging currents. Lifespans of batteries reduce significantly with drawing large currents from them and recharging them by supplying large charging currents. Studies show that charging/discharging batteries at high charging/discharging currents such 4C and 5C reduce the capacities of batteries drastically [14]. Generally, large currents increase the internal resistance of the battery which eventually fades its capacity.

In power systems, batteries are of high energy ratings. As a result, discharging batteries at high currents such as 4C and 5C are impractical due to the currents carrying capacity limitations of power conductors. In addition, current supplied depends on the loads connected to the distribution system. Generally, battery designers calculate the capacity fade at different magnitudes of fixed currents in different experiments. Because of varying magnitudes of load currents in power systems, we use the capacity fade values at the maximum supplied load currents. For a particular value of maximum current, if we know the capacity fade at that current, we can calculate the new capacity of the battery using (5).

$$Q_{NI} = (1-\Psi_I)\times Q_r \Big|_{I=I_{Batt.max}} \quad (5)$$

Where ‘ Q_{NI} ’, ‘ Ψ_I ’ and ‘ $I_{Batt.max}$ ’ are the new rated capacity of a battery after current fading effect, capacity fade effect of current and maximum current supplied by the battery, respectively. ‘ Ψ_I ’ is measured in percentage.

D. Voltage Regulation

When the PV panels and wind DGs generate more power than the power demands, a BESS charges its battery, whereas when the voltage of the system goes below the set limit, a BESS discharges its battery. The charging and discharging power can be obtained from (6) and (7).

$$P_{CHR} = P_{R.CHGR} \quad (6)$$

$$P_{DIS} = P_j + (\chi_{ij}\times Q_j) - \frac{(\Delta V \times V_i)}{R_i} \quad (7)$$

$$\Delta V = (V_{i-1} - V_i),\ \chi_{ij} = \frac{X_{ij}}{R_{ij}} \quad (8)$$

$$I_{Batt} = \left(\frac{P_{DIS/CHR}}{V_i}\right) \quad (9)$$

Where ‘ P_{CHR} ’, ‘ $P_{R.CHGR}$ ’, ‘ P_{DIS} ’, ‘ X_{ij} ’, ‘ R_{ij} ’ and ‘ V_i ’ are the power required for charging the battery, rated capacity of the battery charger, power discharged by the battery, reactance between buses ‘*i*’ and ‘*j*’, resistance between buses ‘*i*’ and ‘*j*’ and voltage of the *i*-th bus, respectively. ‘ P_{CHR} ’, ‘ $P_{R.CHGR}$ ’ and ‘ P_{DIS} ’ are measured in kWs.

The control given in (10) is used for the voltage regulation of a distribution network using a BESS.

$$P_{Batt} = \begin{cases} P_{CHR} & \text{for } V_{(i)} > U.B. \\ P_{DIS} & \text{for } V_{(i)} < L.B. \\ 0 & \text{otherwise} \end{cases} \quad (10)$$

Where ‘ P_{Batt} ’, ‘ $U.B.$ ’ and ‘ $L.B.$ ’ are the power supplied/provided by/to the battery, upper bound and the lower bound values of the voltage, respectively.

III. Problem Formulation for optimization

In this study, the problem of optimal sizing and allocation of the BESS is designed as a multi-objective optimization problem. The first objective function depicts the total energy losses of the system, whereas the second objective function presents the total cost associated with the installation of a BESS. The total cost of a BESS is equal the sum of the costs of battery units, thermal management units, power conditioning units and battery installations.

$$Min\ f_1 = \left(\sum_{h=1}^{D}\sum_{m=1}^{H}\sum_{i=1}^{N}\left(\frac{P_{(i,m,h)}+Q_{(i,m,h)}}{V_{(i,m,h)}}\right)^2 \times R_{(ij)}\right) \quad (10)$$

$$Min\ f_2 = \sum_{i=1}^{N}\left(C_{BU(i)} + C_{TMU(i)} + C_{PE(i)} + C_{INB(i)}\right) \quad (11)$$

Where ‘ f_1 ’, ‘ f_2 ’, ‘ $P_{(i,m,h)}$ ’, ‘ $Q_{(i,m,h)}$ ’, ‘ $C_{BU(i)}$ ’, ‘ $C_{TMU(i)}$ ’, ‘ $C_{PE(i)}$ ’ and ‘ $C_{INB(i)}$ ’ are the functions to be minimized, active and reactive power flowing between buses ‘*i*’ and ‘*j*’, costs of the battery unit, thermal management units, power conditioning units and battery installations, respectively. The U.S. dollar is used as the measuring units for the cost.

A. Constraints

Optimal solution generated must satisfy following constraints imposed to generate feasible solutions.

1) Voltage: The voltage of the *i*-th bus should be within defined minimum and maximum voltage limit.

$$V_{min} \le V_{(i)} \le V_{max} \quad (11)$$

2) Current: The maximum value of current flowing between buses ‘*i*’ and ‘*j*’ should be less than the maximum current carrying capacity of power conductors.

$$|I_{ij}| \le I_{max} \quad (12)$$

3) Maximum number of BESS units: The maximum number of BESS units installed should be less than the allowed units in order to prevent the installation of numerous small size units.

$$\sum_{i=1}^{N} bp_{(i)} \le N_{mb.DG} \quad (13)$$

Where ‘ $bp_{(i)}$ ’ and ‘ $N_{mb.DG}$ ’ are the indication constant that takes value 0 or 1 and maximum numbers of allowed BESS units, respectively.

4) Buses for BESS-placement: The solutions generated for the bus numbers should be the bus number which is the part of the distribution system.

$$P_{(i)}^{B.DG} = 0 \quad \forall\, i \notin BDG \tag{14}$$

Where ‘ $P_{(i)}^{B.DG}$ ’ and ‘ BDG ’ are the rated power of a BESS unit and set of buses for BESS placement, respectively.

5) DOD Limit: DOD of a BESS unit should be within specified minimum and maximum value of the DOD at the end of the simulations.

$$DOD_{min} \le DOD_r \le DOD_{max} \tag{15}$$

B. Total cost savings

If the lifespan a BESS battery is maximized, costs of thermal management units, power conditioning units and installations of BESSs can be saved annually. The cost savings are calculated using (16).

$$TCS = \sum_{y=1}^{Yrs}\sum_{i=1}^{N}\left(C_{TMU(i,y)} + C_{PE(i,y)} + C_{INB(i,y)}\right) \qquad (16)$$

Where ‘ TCS ’ is the total cost saved annually.

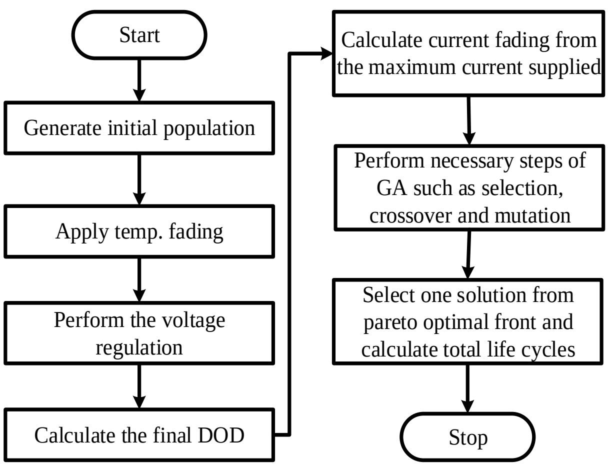

Fig. 3. Steps performed in the proposed scheme

C. Non-dominated sorting genetic algorithm-II (NSGA-II)

In this study, we use a multi-objective evolutionary algorithm, NSGA-II, to solve the optimization problem [15]. At the end of simulations, the solutions are obtained in the form of a pareto optimal set. In the pareto optimal set, no solution is better than the other solution in both objective functions, and the decision of selecting one solution is made on the basis of high level information or available resources. However, there exist some methods in which a compromise solution can be selected from the pareto optimal set. Here, we use one such method for selecting a compromise solution from the pareto optimal set. This method is known as utopian point method. A utopian point is a solution which minimizes both objective functions at the same time, and a compromise solution is found by minimizing Euclidean distance between a utopian point and a pareto optimal front using (16) [16]. Before the value of Euclidean distance is calculated, both objective functions should be normalized.

$$D(x) = \sqrt{\sum_{m=1}^{N}\left(f_m(\mathbf{x}) - \overline{z}_m\right)^2} \qquad (16)$$

Where ‘ $D(x)$ ’ and ‘ $\overline{z}_m$ ’ are the Euclidean distance and a utopian point.

In order to make the optimal sizing and allocation of BESSs, the complete steps performed in the algorithm are given in Fig. 3. First, the algorithm generates the population of random solutions. Second, it applies the capacity fading at the particular temperature and performs the voltage regulation. In case of any constraint violation, it performs the constraint handling procedure. Third, it records the final DOD and calculates the maximum current supplied by the battery. The algorithm runs until the stopping conditions are met, and finally, one solution is selected from the pareto optimal curve. The lifecycles and total savings are then found for that solution.

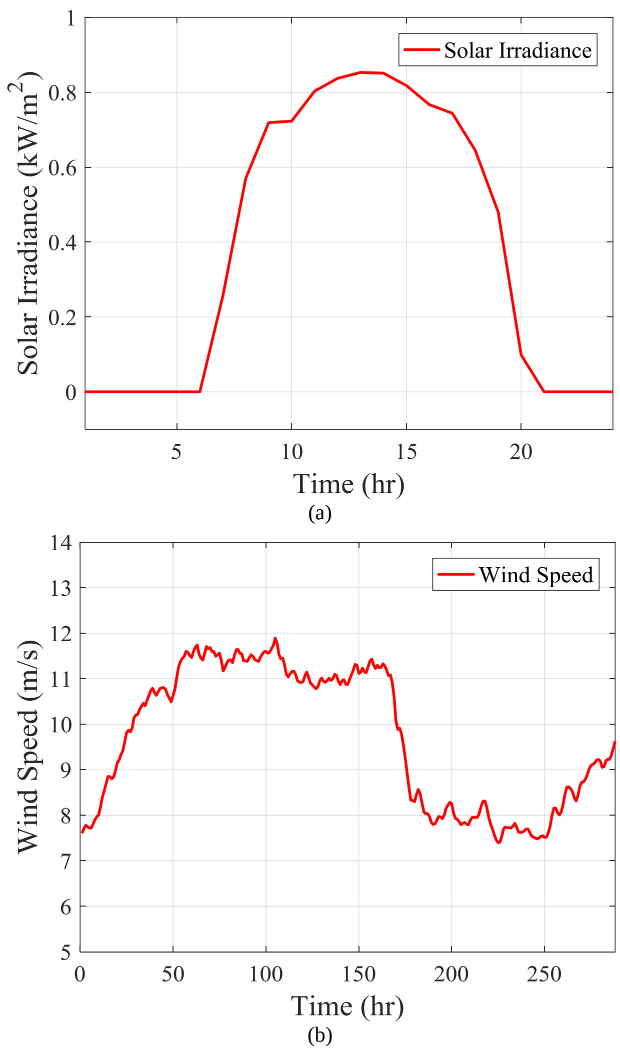

Fig. 4. (a) Solar irradiance (b) Wind speed

IV. TEST SYSTEM AND TEST CASES

In this paper, an IEEE 906-bus test system has been used for the simulations [17]. The BESSs possess Li-ion battery. The parameters of a PV panels and a wind turbine are given in Tables I and II., whereas the costs associated with different parameters of a BESS are given in Table III. A solar irradiance and wind speed profile of a summer day are displayed in Figs. 4a and 4b. The load profile of 24 h has also been considered for the simulations. The details of the load profile can be obtained from [15]. Furthermore, two test cases have been considered. In the first case, the optimal location and sizing of BESSs are found with the PV panels, whereas in the second case, wind power DGs have been placed in the test system to calculate the size and location of BESSs. The ratings of two PV panels installed are 6.5 and 7 kWs, whereas the ratings of both wind power DGs are 5 kWs. Also, in base case 1, only PV panels are operating in the distribution network, whereas in base case 2, only wind DGs are present in the distribution network.

TABLE I
PV MODULE PARAMETERS

Characteristics	Values
Watt peak (W)	75.00
Open circuit voltage (V)	21.98
Short circuit current (A)	5.32
Voltage at maximum power (V)	17.32
Current at maximum power (A)	4.76
Voltage temperature coefficient (mV/°C)	14.40
Current temperature coefficient (mA/°C)	1.22
Nominal cell operating temperature (°C)	43.00

TABLE II
WIND TURBINE PARAMETERS

Characteristics	Values
Cut-in speed (m/s)	4.00
Rated speed (m/s)	14.00
Cut-out speed	25.00

V. RESULTS AND DISCUSSION

Table IV shows the results obtained from the optimization algorithm. The optimal size and location of installation of BESSs are tabulated in Table IV. It is interesting to note that in the base case 1, the losses of the system were 148 kWh, and in the base case 2, the losses were 132 kWh. However, after the placement of BESSs optimally, the losses of the system have been lowered to 115 and 113 kWhs. Generally, the systems with only PV panels have more losses in comparison with those having wind power DGs due to the fact that the solar energy is only available during the day time. However, the wind energy with a variation in its magnitude is available all the day. The cost of the installation has also been provided in Table IV. In addition, the percentage loss reduction shows the comparison of test cases with base cases in terms of loss reductions. The losses in both cases have been reduced.

The voltage profiles of the test feeder are given in Fig. 5. From both figures, it can be noticed that the voltage profile of the system has been improved. The frequent fluctuations, that can be seen in the voltage, are caused by switching in the load as the load switchings in the LV systems are more frequent. The set points of the BESSs were set to 1 p.u. Since PV panels do not provide power at night hours, the sizes of BESSs integrated with them are large as the BESSs have to support the grid during night hours. Whenever, voltage goes above or below 1 p.u., BESSs charge or discharge its battery accordingly. Fig. 6 illustrate the DOD curves of the BESSs over the operation of a whole day. When the excessive power is available, the DOD levels are reduced as the BESSs charge their batteries at that time.

TABLE III
PV MODULE PARAMETERS

Parameters	Values($/kWh)
C_{BU}	300
C_{TMU}	100
C_{PE}	210
C_{INB}	150
DOD_{ini}	0.20
$DOD_{cuttoff}$	0.05
$P_{R.CHGR}$	7 KW
Life cycles	2000 @ 80.0% DOD

TABLE IV
RESULTS OBTAINED FROM NSGA-II

Bus No.	Case-1	Case-2
440	31 kWh	—
277	55 kWh	—
357	—	21 kWh
131	—	42 kWh
Losses(kWh)	**115**	**113**
Cost	**65713**	**48919**
%age Loss Reduction	**22.30**	**14.42**

TABLE V
RESULTS OBTAINED FROM NSGA-II

Case No.	Battery Rating	Life Cycles	Years	Cost Savings ($)
1	31	4,552	12.47	179,135
1	55	4,129	11.31	287,510
2	21	4,275	11.71	116,467
2	42	4,820	13.20	259,706

Finally, in Table V, extension in the lifespan of batteries and annual savings achieved from them are presented. It has been demonstrated that the cost can be saved if the lifespans of the batteries are extended. Interestingly, the increase in lifespan of a battery will not require change of battery every year. Furthermore, this will save the cost associated with the installation, power conditioning units and thermal management units of batteries. It is worth mentioning that the lifecycles obtained and life in year would only be achieved in practice if the BESS units are charged and discharged according to DOD curves shown in Fig.6. All the results presented suggest that the method proposed in this paper can be used to optimally plan the installation of BESSs in order to

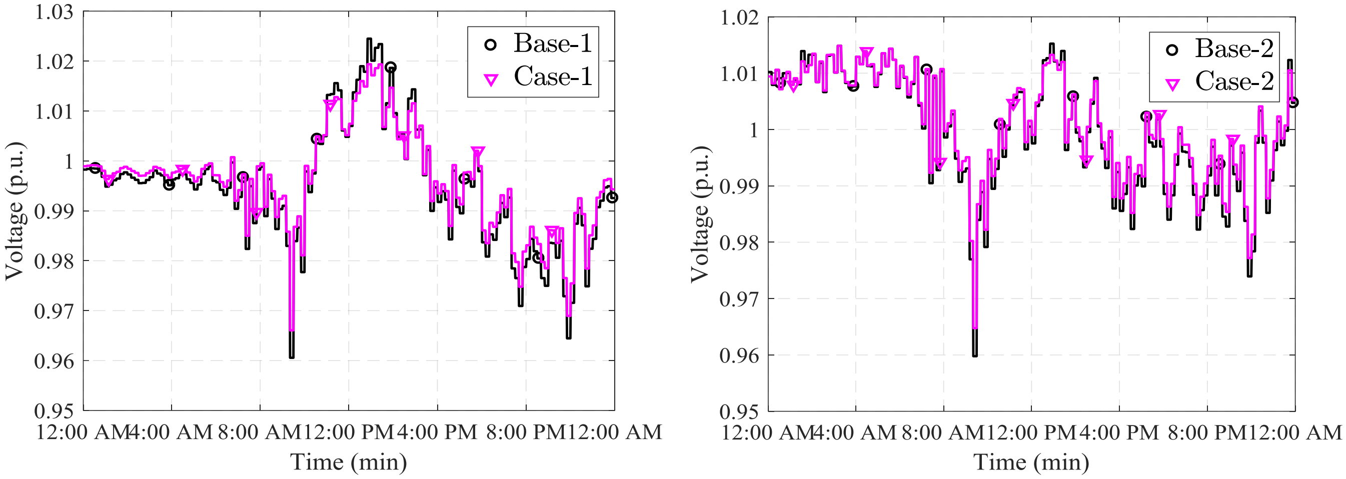

(a) (b)

Fig. 5. Voltage at bus-800 after BESS-placement. (a) Case 1 (b) Case 2.

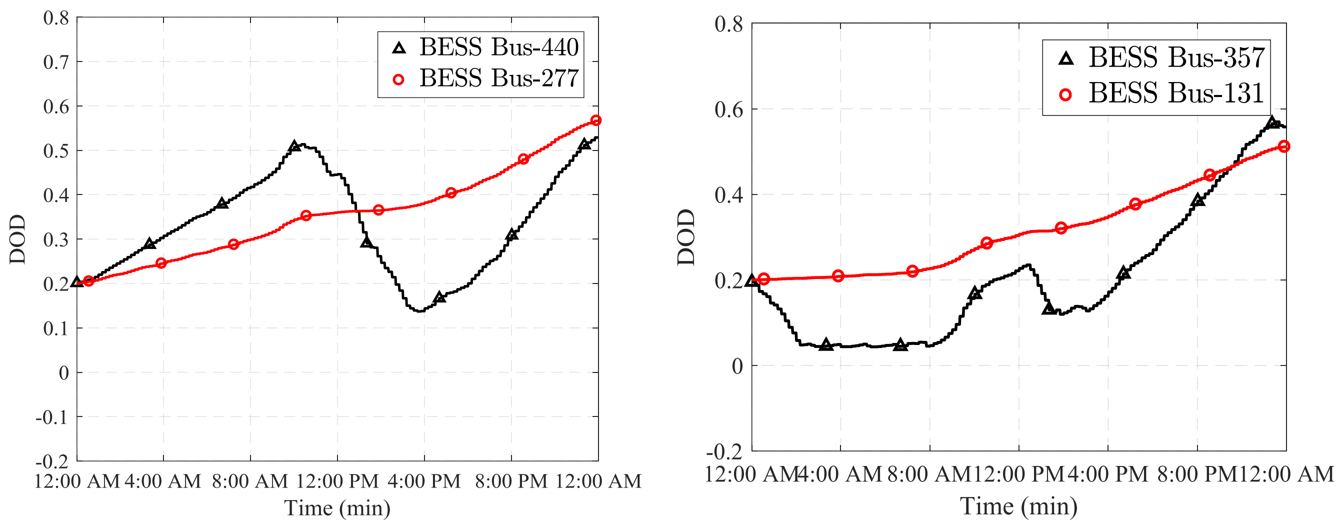

(a) (b)

Fig. 6. DOD curves of BESSs. (a) Case 1 (b) Case 2.

maximize their benefits. Also, it may help in reduction of losses of the system to improve the voltage profile of the distribution networks.

VI. Conclusion

In this paper, a new methodology for optimal sizing and allocation of a BESS was proposed. Various factors such as the operating temperature, the level of DOD, the magnitude of charging/discharging current etc., that affect the lifespan of a BESS battery were considered and modelled. The problem was formulated as a multi-objective optimization problem; the first objective function represented the total energy losses, whereas the second objective function depicted the total cost of installation of BESSs. The voltage regulation algorithm was also integrated with the optimization algorithm. The results showed the reduced losses and costs, and the voltage profile of the distribution network was also improved at the same time. The cost was also saved from the extension in the lifespans of batteries. The results obtained suggest that the proposed study can be employed to maximize the benefits of BESSs, and the cost of annual replacement of batteries can also be reduced using the scheme.

VII. References

[1] Y. Wang, K. T. Tan, X. Y. Peng and P. L. So, "Coordinated Control of Distributed Energy-Storage Systems for Voltage Regulation in Distribution Networks," *IEEE Transactions on Power Delivery*, vol. 31, no. 3, pp. 1132-1141, June 2016.

[2] S. Grillo, M. Marinelli, S. Massucco and F. Silvestro, "Optimal Management Strategy of a Battery-Based Storage System to Improve Renewable Energy Integration in Distribution Networks," *IEEE Transactions on Smart Grid*, vol. 3, no. 2, pp. 950-958, June 2012.

[3] I. Serban and C. Marinescu, "Control Strategy of Three-Phase Battery Energy Storage Systems for Frequency Support in Microgrids and with Uninterrupted Supply of Local Loads," *IEEE Transactions on Power Electronics*, vol. 29, no. 9, pp. 5010-5020, Sept. 2014.

[4] Y. M. Atwa and E. F. El-Saadany, "Optimal Allocation of ESS in Distribution Systems with a High Penetration of Wind Energy," *IEEE Transactions on Power Systems*, vol. 25, no. 4, pp. 1815-1822, Nov. 2010.

[5] C. Chen and S. Duan, "Optimal allocation of distributed generation and energy storage system in microgrids," *IET Renewable Power Generation*, vol. 8, no. 6, pp. 581-589, August 2014.

[6] Y. Zhang, Z. Y. Dong, F. Luo, Y. Zheng, K. Meng and K. P. Wong, "Optimal allocation of battery energy storage systems in distribution networks with high wind power penetration," *IET Renewable Power Generation*, vol. 10, no. 8, pp. 1105-1113, Nov. 2016.
[7] M. Sedghi, A. Ahmadian and M. Aliakbar-Golkar, "Optimal Storage Planning in Active Distribution Network Considering Uncertainty of Wind Power Distributed Generation," *IEEE Transactions on Power Systems*, vol. 31, no. 1, pp. 304-316, Jan. 2016.
[8] S. Sharma, S. Bhattacharjee, and A. Bhattacharya, “Grey wolf optimization for optimal sizing of battery energy storage device to minimize operation cost of microgrid,” *IET Generation, Transmission Distribution*, vol. 10, no. 3, pp. 625–637, 2016.
[9] T. Y. Lee and N. Chen, "Determination of optimal contract capacities and optimal sizes of battery energy storage systems for time-of-use rates industrial customers," *IEEE Transactions on Energy Conversion*, vol. 10, no. 3, pp. 562-568, Sep 1995.
[10] G. Carpinelli, F. Mottola and D. Proto, Probabilistic sizing of battery energy storage when time-of-use pricing is applied, *Electric Power Systems Research*, vol. 141, pp. 73–83, Dec. 2016.
[11] T.M. Bandhauer, S. Garimella, and T.F. Fuller, “A critical review of thermal issues in lithium-ion batteries”, *Journ. Electrochem. Society*, vol. 158, no. 3, pp. R1–R25, 2011.
[12] H. de Vries, T. T. Nguyen, and B. O. het Veld, “Increasing the cycle life of lithium ion cells by partial state of charge cycling,” *Microelectronics Reliability*, vol. 55, no. 11, pp. 2247 – 2253, 2015.
[13] K. S. Ng, C.-S. Moo, Y.-P. Chen, and Y.-C. Hsieh, “Enhanced coulomb counting method for estimating state-of-charge and state-of-health of lithium-ion batteries,” *Applied Energy*, vol. 86, no. 9, pp. 1506 – 1511, 2009.
[14] D. Ansen, M. Dubarry, A. Devie, B. Liaw, V. Garca, J. Viera, and M. Gonzlez, “Fast charging technique for high power lifepo4 batteries: A mechanistic analysis of aging,” *Journal of Power Sources*, vol. 321, pp. 201 – 209, 2016.
[15] K. Deb, A. Pratap, S. Agarwal, and T. Meyarivan, “A fast and elitist multiobjective genetic algorithm: Nsga-ii,” *IEEE Transactions on Evolutionary Computation*, vol. 6, no. 2, pp. 182–197, Apr 2002.
[16] J. S. Arora, Ed., Introduction to Optimum Design, 3rd ed. Boston: Academic Press, 2012.
[17] Distribution test feeders. [Online]. Available: http://ewh.ieee.org/soc/pes/dsacom/testfeeders/index.html